Thermal Resistance of Enclosed Reflective Airspaces in Building Applications*

Hamed H. Saber[#]

Construction Portfolio, National Research Council Canada
Bldg. M-24, 1200 Montreal Road, Ottawa, Ontario, Canada K1A 0R6

Abstract

Many parts of the building envelopes contain enclosed airspaces. The thermal resistance (R-value) of an enclosed airspace depends on the emissivity of all surfaces that bound the airspace, the size and orientation of the airspace, the direction of heat transfer through the airspace, and the respective temperatures of all surfaces that define the airspace. Assessing the energy performance of building envelopes requires accurate determination of the R-values of enclosed airspaces. In this paper, a comprehensive review about the thermal performance of enclosed airspaces is conducted. This review includes the computational and experimental methods for determining the effective R-value of enclosed reflective airspaces. Also, the different parameters that affect the thermal performance of enclosed airspaces are discussed. Finally, practical correlation for determining the R-values of enclosed airspaces of different inclination angels and directions of heat flow as a function of all parameters that affect the thermal performance of the enclosed airspaces, namely: average temperature, temperature differential, aspect ratio, and effective emittance is provided. This correlation can be used by modellers, building designers and architects in the design for thermal resistance of building enclosures. As well, this correlation can be implemented in the currently available energy simulation models (e.g. ESP-r, Energy Plus, DOE, etc.).

Keywords: Reflective insulation, low emissivity material, thermal modelling, R-value correlation, airflow in enclosed airspace, and heat transfer by convection, conduction & radiation.

Introduction

In regions with harsh climatic conditions, a substantial share of energy is used for heating and cooling the buildings [1]. Energy consumption of the building sector is high and although the situation differs from country to country, buildings are responsible for about 30-40% of the total energy demand [2]. In Europe, however, buildings are responsible for 40-50% of energy use and the largest share of energy in buildings is used for heating [3]. The design of building enclosures with the intent of achieving energy savings can necessarily help reduce building operating loads and thus the demand for energy over time [4, 5]. Thermal insulations are major contributors and obviously a practical and logical first step towards achieving energy efficiency especially in buildings located in sites with harsh climatic conditions. This can evidently be achieved by increasing the effective thermal resistance (R-value) of the building envelope.

* Invited paper for Building Enclosure Science & Technology Conference (BEST4) conference. This paper is prepared for publication in the Journal of Building Physics and will also be placed in the BEST 4 proceeding in its pre-print version.

Corresponding author, email: hamed.saber@nrc-cnrc.gc.ca, phone: +1 (613) 993-9772.

Reflective Insulation (RI) products are typically being used in conjunction with mass insulation products, such as glass fibre, expanded polystyrene foam (EPS), and other similar insulation products. The RI products were introduced onto the building market as a promising thermal insulation material. According to the installation guidelines of the Reflective Insulation Manufacturers Association International (RIMA-I) [6], RI products have at least one reflective surface facing an airspace. The RI products can be installed in wall cavities, between ceiling and floor joists, and in metallic buildings that cannot readily accommodate loose-fill or batt-type insulations. Also, RI products can be used as part of a roofing system either below the decking between rafters, within small air gaps between decking and roofing, and in air gaps created, for example, by paneling interior masonry walls [7].

A review about the use of reflective materials to reduce heat transfer by radiation across enclosed airspaces was conducted by Gross and Miller [8]. Fricker and Yarbrough [9] conducted literature review on four computational methods for evaluating the R-values of enclosed reflective airspaces. Those four methods involved an assumption of one-dimensional heat transfer between large parallel surfaces (infinite parallel planes). In an actual building enclosure, however, there are surfaces connecting the parallel planes (e.g. framing). These surfaces absorb, emit and reflect thermal radiation. Glicksman [10] has shown that the heat transfer process that included radiation interaction between the parallel surfaces and the framing resulted in a decrease in the overall thermal performance (i.e. lower R-values).

It is important to accurately determine the effective R-values of the airspaces of different dimensions, effective emittances, inclination angles, directions of heat flow, mean airspace temperatures, and temperature differences across the airspaces. Many studies were conducted to determine the R-values of RI products, and wall and roofing systems incorporating RI products [2-3, 7, 11-31]. Also, there are many claims indicating that RI products can have high thermal resistance. Debate is still ongoing into whether these claims are correct [26]. However, some in situ measurements, and hot box and hot plate measurements performed in laboratories resulted in lower R-values. For example, Saber [22] and Saber et al. [23] showed that a heat flow meter in accordance with standard ASTM C-518 [33] underestimates the effective R-value of RI products that include radiation shields in combination with horizontal enclosed airspaces. The main reason lies in non-uniform convective flows in these airspaces. As such, Tenpierik and Hasselaar [26] conducted an extensive literature review to identify the causes for the different results among different research organizations. D'Orazio et al. [20] conducted field study under hot climatic conditions to investigate the thermal performance of an insulated roof with RI product. The results of that study showed that the benefits of RI product are quite limited when using the insulation level imposed by actual laws, which consider insulation as the main strategy for energy saving in temperate and hot climates.

This paper focuses on the thermal performance of enclosed airspaces under different operation conditions. Note that the term "enclosed" is critical since the major distinction between RIs and Radiant Barriers (RBs) is the airspace condition, where the RB system is defined as a building construction that consists of a low emittance surface bounded by an "open" airspace [1, 11, 13, 15]. The parameters that affect the R-value of an enclosed airspace are: (a) the physical properties of the air filling the space, (b) temperature of all surfaces of the airspace, (c) emissivity of all surfaces of the airspace, (d) temperature differences across the airspace, (e) dimensions of the airspace, (f) direction of heat flow through the airspace, and (g) orientation of the airspace. The R-values of enclosed airspaces were calculated by many investigators (e.g. see Robinson et al. [34, 35, 36] for various orientations of airspaces and reflective boundaries by using heat transfer coefficient data). The heat transfer coefficient data were obtained from measurements of panels of different thicknesses using the test method described in the ASTM C236-53 [37]. In those studies, the steady-state heat transmission rates were corrected for heat transfer occurring along parallel paths between hot and cold boundaries. Thereafter, the convective heat transfer coefficients were obtained from the data by subtracting a calculated radiative heat transfer rate from the total corrected heat transfer rate; and the radiative heat transfer was calculated using an emissivity of 0.028 for the aluminum surfaces.

Generally, the value for the effective heat conductance, U-value (the reciprocal of the R-value) of an enclosed airspace accounts for the contribution of heat transfer in the enclosed space due to heat transfer by conduction, convection and radiation. In the absence of heat transfer by radiation, the contribution of heat transfer by convection in an enclosed space is normally given in terms of the Nusselt number, Nu (Nu = h δ/λ, where h is convective heat transfer coefficient, δ is the thickness of the space, and λ is the thermal conductivity of the fluid filling the space). According to many authors [38 and 39], the convective heat transfer coefficient for an enclosed space can be given as:

$$Nu = h\,\delta/\lambda = a\,(Gr\,.\,\mathrm{Pr})^b A_R^c = a\,(Ra)^b A_R^c, \text{ and } Gr = g\;\beta\;\rho^2\;\delta^3\;\Delta T/\mu^2. \qquad (1)$$

Where the coefficients a, b and c in Eq. (1) are dimensionless constants, derived from experiments, A_R is the aspect ratio of the enclosed space (A_R = height (H)/thickness (δ)), Gr is the Grashoff number, Ra is the Raleigh number (Ra = Gr.Pr), Pr is the Prandtl number, g is the gravitational acceleration, β is the thermal expansion coefficient, ρ is the density, and μ is the dynamic viscosity. In order to derive the coefficients a, b and c (Eq. (1)) from which the heat transfer coefficient, h, due to the convective component of heat transfer can be determined, the emissivity of all surfaces that bound the enclosed space must be zero (i.e. purely reflective surfaces). However, it is not possible in practice to use materials having zero emissivity when conducting such experiments. Hence, to derive the coefficients a, b and c of Eq. (1) from experiments, as mentioned previously, the rate of radiative heat transfer across the enclosed space would be subtracted from the total rate of heat transfer across the space.

A number of correlations for the value of Nu in the form of the relationship given in Eq. (1) and for different ranges of values of Ra, A_R and Pr are provided in several studies as described in the IEA Annex XII report [38]. Some of these correlations showed the dependence of the Nu on the aspect ratio of the enclosed space (A_R). As such, it is anticipated that the effective thermal conductance or the effective thermal resistance of the enclosed space would be affected by the aspect ratio of the enclosed space, as will be shown later.

The 2009 ASHRAE Handbook of Fundamentals, Chapter 26 [40] provides a table that contains the R-values for enclosed airspaces of three inclination angles (θ) of 0^o, 45^o and 90^o, which were determined on the basis of the heat transfer data reported by Robinson et al. [34, 35, 36]. These R-values are being extensively used by modellers, architects and building designers to determine the R-values of building enclosures. The ASHRAE R-values were obtained by combining the convective and radiative components of heat transfer from which the effective R-value for an enclosed airspace was provided for airspaces of different: (a) thickness (δ = 13 mm (0.5 in), 20 mm (0.75 in), 40 mm (1.5 in), and 90 mm (3.5 in)), (b) mean temperature (T_{avg} = 32.2^{o}C (90^{o}F), 10.0^{o}C (50^{o}F), -17.8^{o}C (0^{o}F) and -45.6^{o}C (-50^{o}F)), (c) temperature difference across the airspace (ΔT = 5.6^{o}C (10^{o}F), 11.1^{o}C (20^{o}F) and 16.7^{o}C (30^{o}F)), (d) effective emittance (ε_{eff} = 0.03, 0.05, 0.2, 0.5 and 0.82), and (e) direction of heat flow through the airspace. Note that the effective emittance (ε_{eff}) of an enclosed airspace is given as [40]:

$$1/\varepsilon_{eff} = 1/\varepsilon_1 + 1/\varepsilon_2 - 1, \qquad (2)$$

where ε_1 and ε_2 are the emissivity of the hot and cold surfaces (see Figure 1a). It is worth mentioning that the R-values of low-sloped enclosed airspaces are not available in the ASHRAE table. As well, the effect of the aspect ratio (length/thickness) of the enclosed airspace on the R-values is not accounted for in the ASHRAE table [40].

In recent studies by the author [28 – 32], the NRC's hygrothermal model, called hygIRC-C, was used to predict the R-values of vertical, horizontal, high-sloped (45^o) and low-sloped (30^o) enclosed airspaces for a wide range of airspace different thickness, aspect ratio, mean temperature, temperature differential, effective emittance, and direction of heat flow. In those studies [28 – 32], considerations were also given to investigate the potential increase in the R-value of the enclosed airspace when a thin sheet having different values of emissivity on both sides was placed in the middle of the airspace as shown in Figure 1b. The results showed that, depending on the value of the effective emittance, the thickness of the airspace, orientation of the airspace, and the direction of heat flow, the R-value could be tripled by incorporating this thin sheet along the middle of the enclosed airspace. The model description and benchmarking are discussed next.

Model Benchmarking

The numerical model, hygIRC-C, that was used to investigate the thermal performance of enclosed airspaces solves simultaneously the 2D and 3D moisture transport equation, energy equation, surface-to-surface radiation equation (e.g. surface-to-surface radiation in enclosed airspace such as shown in Figure 1) and air transport equation in the various material layers. The air transport equation is the Navier-Stokes equation for the airspace (e.g. air cavity), and Darcy equation (Darcy Number, DN $<10^{-6}$) and Brinkman equation (DN $> 10^{-6}$) for the porous material layers (see [4, 5, 18, 19, 23, 24, 41, 42, 43] for more details).

The numerical model had been previously benchmarked in a number of building applications (e.g. see [18, 22, 23, 44]). For the applications that are similar to this study, the numerical model was benchmarked against the thermal performance data for a full-scale wall assembly featuring a reflective insulation product. The data was obtained using a Guarded Hot Box (GHB) in accordance with ASTM C-1363 test method [45]. Results showed that the R-value predicted by the model for this wall system was in good agreement with the measured R-value (within 1.2%) [18, 44]. Furthermore, the numerical model was benchmarked against a number of tests that were conducted at the Cold Climate Housing Research Center (CCHRC) [17] and the National Research Council of Canada (NRC) [22, 23]. These tests were conducted using heat flow meters in accordance with the ASTM C-518 test method [33] to examine the thermal performance of different types of reflective insulation assemblies. The results showed that the heat fluxes predicted by the model were in good agreements with the measured heat fluxes (within $\pm$1.0%). Thereafter, the model was used to investigate the contribution of reflective insulations to the R-value for specimens having three inclination angles (θ = 0^o, 45^o and 90^o), different directions of heat flow through the specimens, and a wide range of foil emissivity [22].

In previous studies, the model was used to determine the R-values of vertical enclosed airspaces (θ = 90^o) [28], horizontal enclosed airspaces (θ = 0^o) with upward heat flow [29] and downward heat flow [31], and high-sloped enclosed airspaces (θ = 45^o) with downward heat flow [30]. In those studies, the predicted R-values were compared with the ASHRAE R-values [40] for enclosed airspaces of different thicknesses and different operating conditions. Also, the model was used to determine the R-values of low-sloped enclosed airspaces (θ = 30^o) and subjected to downward heat flow conditions [32].

For the cases of open and closed airspaces in wall systems, the model was used to determine the effective thermal resistance of a number of foundation wall systems with a low emissivity material bonded to thermal insulation and furred-airspace assembly, and subjected to different climatic conditions of Canada (Toronto, Quebec, Sept-Iles, Ottawa, and Victoria) [47-49]. In that study, for the case of open airspace, the effect of infiltration and exfiltration on the effective R-value was accounted for [47]. A full description of the present model and more details about model benchmarking are available in previous publications [4-5, 16, 18, 19, 21, 23-24, 41-42, 46].

Effect of Inclination Angle and Direction of Heat Flow

As indicated earlier, the reflective insulations are being used in sloped roof systems. In this particular application, it might be difficult to adapt one of the available test methods such as the ASTM C-518 [33] and ASTM C-1363 [45] in order to measure the R-value of specimen with reflective insulation. For instance, the ASTM C-518 test method could be used in the case of specimen with horizontal and vertical orientations only [33]. After gaining confidence in the present model, as described in the previous section, in predicting the R-value of specimen with horizontal orientation (e.g. see [23]) and specimen with vertical orientation (e.g. see [18]), it was used to quantify the contribution of reflective insulation to the R-value of specimen with different orientations.

A parametric study was conducted to investigate the effect of inclination angle (θ) and direction of heat flow on the effective R-value of EPS sample stack shown in Figure 2 [22]. Note that the rate of heat transfer by both convection and radiation in the air cavity depends on its size and the temperature difference across the sample stack (ΔT). As such, the effective R-value depends on both ΔT and the size of the air cavity. The results presented in this section are obtained for *only* one ΔT of 22.4°C (T_c = 12.7°C, and T_h = 35.1°C) and one size of the air cavity as shown in Figure 2.

In the case of foil emissivity of 0.05, Figure 3 and Figure 4 show the vertical velocity (v) and horizontal velocity (u) contours and the airflow field in the cavity for different inclination angles (θ) when the sample stack was heated from the top and the bottom. As shown in these figures, in the case of sample stack heated from the top with θ = 30° and vertical sample stack heated from the left (θ = 90°), a mono-cellular with one vortex cell airflow is developed in the air cavity. In the case of sample stack heated from the bottom with θ = 30°, a multi-cellular airflow is developed in the cavity with three vortex cells. For horizontal sample stack (θ = 0°) heated from the bottom and top, multi-cellular airflow is developed in the cavity with six and two vortex cells, respectively.

Figure 3 and Figure 4 show that the value of the air velocity in the cavity is greatly affected by both θ and direction of heat flow through the sample stack. For horizontal sample stack (θ = 0°), the air velocity in the case of downward heat flow (sample heated from the top, v$\uparrow$(max) = 0.6 mm/s, u$\rightarrow$ (max) = 3.2 mm/s) is much smaller than that in the case of upward heat flow (sample heated from the bottom, v$\uparrow$(max) = 18.7 mm/s, u$\rightarrow$ (max) = 22.1 mm/s). This is due to a downward heat flow encourages a relatively stable stratification of air due to differences in buoyancy compared to the case with upward heat flow. As such, a sample stack with downward heat flow results in a greater R-value (12.19 ft^{2}hr°F/BTU) than that with upward heat flow (10.82 ft^{2}hr°F/BTU) (see Figure 5a). By subtracting the R-value of both the top and bottom EPS layers (8.33 ft^{2}hr°F/BTU) from the total R-value of the sample stack, the middle layer with the air cavity contributed to the R-value by 3.86 ft^{2}hr°F/BTU and by 2.49 ft^{2}hr°F/BTU in the case of horizontal sample stack heated from the top and bottom, respectively (Figure 5b). Similarly, for θ = 30°, the air velocity in the cavity of sample stack heated from the top

($v\uparrow(max)$ = 10.6 mm/s, $u\rightarrow$ (max) = 18.5 mm/s) is also smaller than that heated from the bottom ($v\uparrow(max)$ = 14.1 mm/s, $u\rightarrow$ (max) = 23.3 mm/s). Consequently, the contribution of middle layer with air cavity to the R-value for the former (3.26 ft^2hr^oF/BTU) is greater than that for the latter (2.65 ft^2hr^oF/BTU) (Figure 5b). For vertical sample stack (θ = 90^o) heated from the left or right, the contribution of the middle layer with air cavity to the R-value is 2.63 ft^2hr^oF/BTU.

Figure 6a and Figure 6b show the effect of the foil emissivity on the effective R-value and the contribution of the middle layer with air cavity to the R-value, respectively, for sample stack with different inclination angles and different directions of heat flow. As shown in these figures, for all values of foil emissivity, the horizontal sample stack heated from the top (downward heat flow) resulted in the highest R-values while the horizontal sample stack heated from the bottom (upward heat flow) resulted in the lowest R-values. These two cases, respectively, represent the application of using reflective insulations in flat roof in the summer season and winter season. As provided in references [21-24], the foil emissivity can increase due to oxidation of the foil, accumulation of dust and/or vapor condensation on the surface of the foil. Increasing the foil emissivity from 0.05 to 0.9 resulted in a decrease in the R-value by 20.7% and 8.2% for horizontal sample stack heated from the top and bottom, respectively (Figure 6a). Note that the emissivity of 0.9 represents the case of no foil installed on the system. Moreover, as the foil emissivity increases from 0.05 to 0.9, the contribution of the air cavity to the R-value decreases by 118% (from 3.86 ft^2hr^oF/BTU to 1.77 ft^2hr^oF/BTU) and 49% (from 2.49 ft^2hr^oF/BTU to 1.67 ft^2hr^oF/BTU) for horizontal sample stack heated from the top and bottom, respectively (Figure 6b).

In the case of sample stack with inclination angle of 30^o (e.g. application of reflective insulations in sloped roof), increasing the foil emissivity from 0.05 to 0.9 resulted in a decrease in the R-value by 15.0% and 9.5% for sample stack heated from the top (summer season) and bottom (winter season), respectively (Figure 6a). Also, Figure 6b shows that as the foil emissivity increases from 0.05 to 0.9, the contribution of the air cavity to the R-value decreases by 86% (from 3.26 ft^2hr^oF/BTU to 1.75 ft^2hr^oF/BTU) and 56% (from 2.65 ft^2hr^oF/BTU to 1.70 ft^2hr^oF/BTU) for sample stack heated from the top and bottom, respectively. Furthermore, in the case of vertical sample stack (e.g. application of reflective insulations in wall systems, windows and curtain walls), increasing the foil emissivity from 0.05 to 0.9 resulted in a decrease in the R-value by 11.0% (Figure 6a). In this case the contribution of the air cavity to the R-value decreases by 68% (from 2.81 ft^2hr^oF/BTU to 1.67 ft^2hr^oF/BTU).

In the case of no foil installed in sample stack or the foil surface is fully covered by dust and/or vapor condensation (i.e. ε = 0.9), both inclination angle and direction of heat flow through the specimen have insignificant effect on the effective R-value (i.e. resultant lines tend to converge as ε tends to 0.9, see Figure 6a). In this case, the maximum change in the contribution of air cavity to the R-value is only 6% (from 1.77 ft^2hr^oF/BTU to 1.67 ft^2hr^oF/BTU, Figure 6b). Therefore, for accurate energy calculations for roof and wall systems with reflective insulations, subjected to different climate conditions, it is important to conduct hygrothermal simulations instead of thermal simulations in order to investigate whether or not vapor condensation occurs on the surface of the foil.

Effect of Installing Thin Sheet in the Middle of Enclosed Airspace

Dividing an enclosed airspace into 2 or more cavities by thin sheet(s) would increase the R-value of the enclosed airspace. Figure 1a shows a case of 1-Cavity (i.e. without thin sheet) and Figure 1b shows a case of 2-Cavities (i.e. with thin sheet). A practical example for the case "2-Cavities" is to install a thin sheet with low emissivity at the middle of the enclosed airspace. For the applications of planar skylights, windows and curtain wall systems, the thin sheet should be transparent that can be coated with a transparent material of low emissivity. However, for the applications of wall and roofing systems with enclosed airspaces, the thin sheet could be opaque (e.g. aluminum foil). The benefits of installing a thin sheet are: (a) reducing heat transfer by convection, and (b) reducing heat transfer by radiation due to low effective emittance. These benefits resulted in higher R-value for the "2-Cavities" case compared to the "1-Cavity" case.

In previous studies [28-32], the results showed that the R-value could be doubled due to installing a thin sheet in the middle of: (a) low-sloped enclosed airspaces ($\theta = 30^o$) with downward heat flow [32], (b) high-sloped enclosed airspaces ($\theta = 45^o$) with downward heat flow [30], (c) vertical enclosed airspace ($\theta = 90^o$) [28], and (d) horizontal enclosed airspace ($\theta = 0^o$) with downward heat flow [31]. However, the R-value could be tripled if a thin sheet is installed horizontally in the middle of the horizontal enclosed airspace ($\theta = 0^o$) with upward heat flow condition [29]. These results are important for future applications when a thin reflecting foil is placed in the middle of the enclosed airspace of planar skylights, windows, curtain wall systems, and Furred-Airspace Assemblies (FAA) attached to thermal insulation in wall and roofing systems so as to enhance the energy performance of these systems.

Dependence of the R-value on the Aspect Ratio

In recent studies, the dependence of the R-value on the aspect ratio, A_R (A_R = length (H)/thickness (δ)) of the vertical enclosed airspaces ($\theta = 90^o$) [28], horizontal airspaces ($\theta = 0^o$) with upward heat flow [29] and downward heat flow [31], high-sloped airspaces ($\theta = 45^o$) with downward heat flow [30], and low sloped airspaces ($\theta = 30^o$) with downward heat flow [32] were investigated. Those studies covered a wide range of enclosed airspace: (a) thickness (δ = 13 mm (0.5 in), 20 mm (0.75 in), 40 mm (1.5 in) and 90 mm (3.5 in)), (b) length (H = 203 mm (8 in) – 2438 mm (96 in)), (c) average temperature (T_{avg} = 32.2 (90^{o}F), 10.0^{o}C (50^{o}F), -17.8^{o}C (0^{o}F) and -45.6^{o}C (-50^{o}F)), (d) temperature differential (ΔT = 5.6^{o}C (10^{o}F), 11.1^{o}C (20^{o}F) and 16.7^{o}C (30^{o}F)), and (e) effective emittance (ε_{eff} = 0 – 0.82). The ranges of the aspect ratio in those studies are: A_R = 16 to 188 for δ = 13 mm (0.5 in), A_R = 10 to 122 for δ = 20 mm (0.75 in), A_R = 5 to 61 for δ = 40 mm (1.5 in), and A_R = 2 to 27 for δ = 90 mm (3.5 in). Depending on the thickness of the airspace and the operating conditions, the results of those studies showed that the aspect ratio can have a significant effect on the R-value (see [28-32] for more details). Note that the effect of the airspace aspect ratio and the inclination angle of 30^o on the R-values of enclosed airspaces are not accounted for in the ASHRAE table [40].

Practical Correlation for the R-values of Enclosed Airspaces

Practical correlation was developed in recent studies [28-32] to determine the R-values in (ft^{2}hr^{o}F/BTU) as a function of all parameters that affect the thermal performance of the enclosed airspaces, namely: average temperature (T_{avg}), temperature differential (ΔT), aspect ratio (A_R) and effective emittance (ε_{eff}). The ranges of these parameters cover most of building applications. This correlation is given in the following form:

$$R-value = R_c(T_{avg}) + a_0 A_R^{\alpha_1} T_{avg}^{a_1} \left(\Delta T\right)^{c_1} + a\, \varepsilon_{eff}^{\beta} T_{avg}^{a_2} \left(\Delta T\right)^{c_2} \sum_{i=1}^{4} g_i A_R^i + A_R^{\alpha_2} T_{avg}^{a_3} \left(\Delta T\right)^{c_3} \sum_{i=1}^{4} b_i \varepsilon_{eff}^i \tag{3}$$

In this correlation, $R_c(T_{avg})$ is the R-value in (ft^{2}hr^{o}F/BTU) of the enclosed airspace due to heat transfer by conduction only, which is given as:

$$R_c(T_{avg}) = \delta / \lambda(T_{avg}), \tag{4}$$

where,

$$\lambda(T_{avg}) = \sum_{i=0}^{4} f_i\, T_{avg}^{i},\; f_0 = \text{-}0.00227583562,\; f_1 = 1.15480022 \times 10^{-4},$$
$$f_2 = \text{-}7.90252856 \times 10^{-8},\; f_3 = 4.11702505 \times 10^{-11},\; f_4 = \text{-}7.43864331 \times 10^{-15} \tag{5}$$

Note that $\lambda(T_{avg})$ in Eq. (5) is the average thermal conductivity of air in (W/mK), which is evaluated at the average temperature of the airspace, T_{avg} in (K). It is important to point out that the calculated value of $R_c(T_{avg})$ from Eq. (4) and (5) must be converted to (ft^{2}hr^{o}F/BTU) in order to be used in Eq. (3).

In Eq. (3), the units of T_{avg} and ΔT must be in (K). The other coefficients in this equation ($a_0, a, b_1, b_2, b_3, b_4,\ \alpha_1, \alpha_2, \beta, a_1, a_2, a_3, c_1, c_2, c_3, g_1, g_2, g_3,$ and g_4) are provided in the references [28-32] for enclosed airspace of different inclination angles and directions of heat flow. The results showed that the calculated R-values using Eq. (3) for different inclination angles and directions of heat flow were in good agreements with those obtained using the benchmarked model as described earlier (within ±3% to ±5%; more details are available in [28-32]).

Summary

It is of practical importance in the design of building envelopes to determine the thermal resistance (R-value) of enclosed airspaces of different orientations and directions of heat flow, and having different values of effective emittance under varying climatic conditions as the results of the design may help avoid selecting oversized heating or cooling equipments. In this paper, a comprehensive review about the thermal performance of enclosed airspaces was conducted, which included the computational and experimental methods for determining the effective R-value of enclosed airspaces. The effects of both the inclination angle and direction of heat flow on the thermal performance of enclosed airspaces were discussed. Considerations were given to review the potential increase in the R-value of the enclosed airspace when a thin sheet having different values of emissivity on both sides was placed in the middle of the airspace. Depending on the inclination angle and direction of heat flow of the airspace, the results showed that the R-value could be doubled or tripled by incorporating this thin sheet along the middle of the enclosed airspace. As well, the dependence of the R-value on the aspect ratio of the enclosed airspace was discussed for different conditions. The results showed that the aspect ratio has a significant effect on the R-value.

Practical correlation was provided for determining the R-values of enclosed airspaces of different thicknesses, and for a wide range of values for various parameters, including: (a) aspect ratio, (b) temperature difference across the airspace, (c) mean temperature, and, (d) effective emittance. This correlation is provided by Eq. (3). The calculated R-values using this correlation were in good agreements with the predicted R-values (within ±3% to ±5%). This correlation can be used by architects, modellers and building designers to determine the R-values of enclosed airspaces having wide range of the aspect ratio and effective emittance, and subjected to a wide range of mean temperatures and temperature differences across the airspace. Furthermore, this correlation can be readily implemented in currently available energy simulation models (e.g. ESP-r, Energy Plus, DOE).

References

1. Al-Homoud, M.S., “Performance characteristics and practical applications of common building thermal insulation materials”, *Journal of Building and Environment*, 40: 353–366, 2005, doi:10.1016/j.buildenv.2004.05.013.
2. Vrachopoulos, M.G., Koukou, M.K., Stavlas, D. G., Stamatopoulos, V. N., Gonidis, A.F., and Kravvaritis, E.D., “Testing reflective insulation for improvement of buildings energy efficiency”, *Central European Journal of Engineering,* 2(1): 83-90, 2012, DOI:10.2478/s13531-011-0036-3.
3. European Commission, Green public procurement thermal insulation technical background report. Report for the European Commission – DG Environment by AEA, Harwell, Owner, Editor: European Commission, DG Environment-G2, B-1049, Brussels, 2010.
4. Saber, H.H., Swinton, M.C., Kalinger, P., and Paroli, R.M., “Long-term hygrothermal performance of white and black roofs in North American climates”, *Journal of Building and Environment*, 50: 141-154, 2012, http://dx.doi.org/10.1016/j.buildenv.2011.10.022.
5. Saber, H.H., Swinton, M.C., Kalinger, P., and Paroli, R.M., “Hygrothermal simulations of cool reflective and conventional roofs”, *2011 NRCA International Roofing Symposium, Emerging Technologies and Roof System Performance*, held in Sept. 7-9, 2011, Washington D.C., USA.
6. RIMA-I, Reflective Insulation Manufacturers Association International (RIMA-I), Reflective Insulation, Radiant Barriers and Radiation Control Coatings. Olathe, KS: RIMA-I, 2002.
7. Yarbrough, D., Assessment of reflective insulations for residential and commercial applications. ORNL/TM-8891, Oak Ridge National Laboratory, Oak Ridge, TN. p. 1-63, 1983.
8. Gross, W.P., and Miller, R.G, “Literature review of measurement and predictions of reflective building insulation system performance”, *ASHRAE Transactions*, 95 (2), pp. 651-664, 1989.
9. Fricker, J.M., and Yarbrough, D.W, “Review of reflective insulation estimation methods. Proceedings of Building Simulation”, 12th Conference of International Building Performance Simulation Association, Sydney, 14-16 November 2011, pp. 1989-1996.
10. Glicksman, L. R., “Two-dimensional heat transfer effects on vacuum and reflective insulations”, *Journal of Thermal Insulation,* vol. 14, pp. 281-294, 1991.
11. Fairey, P., “The measured side-by-side performance of attic radiant barrier systems in hot and humid climates”, *19th International Thermal Conductivity Conference*, Cookville, Tenn., pp. 481–496, 1985.
12. Han, B.J., Yarbrough, D.W., and Han, S.M., “Thermal resistance of wall cavities containing reflective insulation”, *Journal of Solar Energy Engineering*, vol.108, pp. 338-341, 1986.
13. Desjarlais, A.O., and Tye, R.P., “Research and development data to define the thermal performance of reflective materials used to conserve energy in building applications”, ORNL/Sub/88-SA835/1, 1990.
14. Desjarlais, A.O., and Yarbrough, D.W., “Predictions of the thermal performance of single and multi-airspace reflective insulation materials”, *ASTM STP 1116*, R.S. Graves and D.C. Wysocki, Eds., American Society for Testing and Materials, pp. 24-43, 1991.
15. Medina, M.A., “On the performance of radiant barriers in combination with different attic insulation levels” *Journal of Energy and Buildings*, 33 (1): 31–40, 2000.
16. Saber, H.H., and Swinton, M.C., “Determining through numerical modeling the effective thermal resistance of a foundation wall system with low emissivity material and furred – airspace”, the *2010 International Conference on Building Envelope Systems and Technologies, ICBEST 2010*, Vancouver, British Colombia, Canada, June 27-30, 2010, pp. 247-257.
17. Craven, C., and Garber-Slaght, R., Product test: reflective insulation in cold climates, Technical Report Number TR 2011-01, Cold Climate Housing Research Center (CCHRC), Fairbanks, AK 99708, 2011, www.cchrc.org.

18. Saber, H.H., Maref, W., Swinton, M.C., and St-Onge, C., "Thermal analysis of above-grade wall assembly with low emissivity materials and furred-airspace", *Journal of Building and Environment*, 46(7): 1403-1414, 2011, doi:10.1016/j.buildenv.2011.01.009.
19. Saber, H.H., Maref, W., and Swinton, M.C., "Numerical investigation of thermal response of basement wall systems with low emissivity material and furred – airspace", *13th Canadian Conference on Building Science and Technology (13th CCBST) Conference*, held in May 10 – 13, 2011 in Winnipeg, Manitoba, Canada.
20. D'Orazio, M., Di Perna, C., Di Giuseppe, E., and Morodo, M., "Thermal performance of an insulated roof with reflective insulation: Field tests under hot climatic conditions" *Journal of Building Physics,* 36 (3), pp. 229–246, 2012, doi:10.1177/1744259112448181.
21. Saber, H.H., and Maref, W., "Effect of furring orientation on thermal response of wall systems with low emissivity material and furred-airspace", *Building Enclosure Science & Technology (BEST3) Conference*, held in April 2-4, 2012 in Atlanta, Georgia, USA.
22. Saber, H.H., "Investigation of thermal performance of reflective insulations for different applications", *Journal of Building and Environment,* 55: 32-44, 2012, doi:10.1016/j.buildenv.2011.12.010.
23. Saber, H.H., Maref, W., Sherrer, G., and Swinton, M.C., "Numerical modeling and experimental investigations of thermal performance of reflective insulations", *Journal of Building Physics,* 36(2): 163-177, 2012, http://dx.doi.org/10.1177/1744259112444021.
24. Saber, H.H., Maref, W., and Swinton, M.C., "Thermal response of basement wall systems with low-emissivity material and furred airspace", *Journal of Building Physics*, 35(4): pp. 353-371, 2012, DOI: 10.1177/1744259111411652.
25. Escudero, C., Martin, K., Erkoreka, A., Floresb, I., and Sala, J.M., "Experimental thermal characterization of radiant barriers for building insulation", *Journal of Energy and Buildings,* vol. 59, pp. 62–72, 2013.
26. Tenpierik, M.J. , and Hasselaar, E., "Reflective multi-foil insulations for buildings: A review", *Journal of Energy and Buildings,* vol. 56, pp. 233–243, 2013.
27. Saber, H.H., "Thermal performance of wall assemblies with low emissivity", *Journal of Building Physics*, 36 (3): 308-329, 2013, DOI: 10.1177/1744259112450419.
28. Saber, H.H., "Practical correlations for the thermal resistance of vertical enclosed airspaces for building applications", *Journal of Building and Environment*, vol. 59, pp. 379-396, 2013, http://dx.doi.org/10.1016/j.buildenv.2012.09.003.
29. Saber, H.H., "Practical correlation for thermal resistance of horizontal enclosed airspaces with upward heat flow for building applications", *Journal of Building and Environment*, vol. 61, pp. 169-187, 2013, http://dx.doi.org/10.1016/j.buildenv.2012.12.016.
30. Saber, H.H., "Practical correlation for thermal resistance of 45^o sloped enclosed airspaces with downward heat flow for building applications", *Journal of Building and Environment*, vol. 65, pp. 154-169, 2013, http://dx.doi.org/10.1016/j.buildenv.2013.04.009.
31. Saber, H.H., "Practical correlation for thermal resistance of horizontal enclosed airspaces with downward heat flow for building applications", *Journal of Building Physics*, vol. 37 (4), pp. 403-435, 2014, http://jen.sagepub.com/content/early/2013/08/19/1744259113498473.
32. Saber, H.H., "Practical correlation for thermal resistance of low-sloped enclosed airspaces with downward heat flow for building applications", *HVAC&R Research Journal*, 20 (1), pp. 92-112, 2014, http://dx.doi.org/10.1080/10789669.2013.834779.
33. ASTM, ASTM C-518: Standard test method for steady-state heat flux measurements and thermal transmission properties by means of the heat flow meter apparatus, Annual Book of Standards, 04.06, 153-164, 2003, American Society for Testing and Materials, Philadelphia, Pa, www.astm.org.

34. Robinson, H.E., Cosgrove, L.A., and Powell, F.J., Thermal resistance of airspaces and fibrous insulations bounded by reflective airspace. Building Material and Structures Report 151, United States National Bureau of Standards, 1956.
35. Robinson, H.E., and Powlitch, F.J., “The thermal insulating value of airspaces”, Housing Research Paper No. 32, National Bureau of Standards Project ME-12, U.S. Government Printing Office, Washington, D.C., 1954.
36. Robinson, H.E., Powlitch, F.J., and Dill, R.S., “The thermal insulation value of airspaces”, Housing Research Paper 32, Housing and Home Finance Agency, 1954.
37. ASTM, ASTM C236-53: Test method for thermal conductance and transmittance of built-up sections by means of a guarded hot box, American Society for Testing and Materials, 1953.
38. IEA Annex XII, International Energy Agency, Energy Conservation in Buildings and Community Systems Programme, Annex XII, Windows and Fenestration, Step 2, Thermal and Solar Properties of Windows, Expert Guide, December, 1987.
39. Saber, H.H., and Laouadi, A., “Convective heat transfer in hemispherical cavities with planar inner surfaces (1415-RP)”, Journal of ASHRAE Transactions, Volume 117, Part 2, 2011.
40. ASHRAE, *2009 ASHRAE Handbook – Fundamentals*, Chapter 26: Heat, air, and moisture control in building assemblies – material properties., SI Edition. Atlanta, GA: American Society of Heating, Refrigeration and Air-Conditioning Engineers, Inc., 2009.
41. Saber, H.H., Maref, W., Elmahdy, A.H., Swinton, M.C., and Glazer, R., “3D thermal model for predicting the thermal resistances of spray polyurethane foam wall assemblies”, *Building XI Conference*, December 5-9, 2010, Clearwater Beach, Florida, USA.
42. Saber, H.H., Maref, W., Lacasse, M.A., Swinton, M.C., Kumaran, M.K., “Benchmarking of hygrothermal model against measurements of drying of full-scale wall assemblies”, *2010 International Conference on Building Envelope Systems and Technologies, ICBEST 2010*, Vancouver, British Colombia, Canada, June 27-30, 2010, pp. 369-377.
43. Saber, H.H., Maref, W., Elmahdy, A.H., Swinton, M.C., and Glazer, R., 3D heat and air transport model for predicting the thermal resistances of insulated wall assemblies. *International Journal of Building Performance Simulation*, 5(2): 75–91, 2012, http://dx.doi.org/10.1080/19401493.2010.532568.
44. Air-Ins Inc., Performance evaluation of Enermax product tested for CCMC evaluation purposes as per CCMC technical guide master format 07 21 31.04, Confidential Test Report Prepared for Products of Canada Corp., AS-00202-C, August 17th, 2009.
45. ASTM, ASTM C-1363: Standard test method for the thermal performance of building assemblies by means of a hot box apparatus, 2006 Annual Book of ASTM Standards 04.06:717–59, www.astm.org.
46. Elmahdy, A.H., Maref, W., Swinton, M.C., Saber, H.H., and Glazer, R., “Development of energy ratings for insulated wall assemblies”, *2009 Building Envelope Symposium,* held in San Diego, CA, October, 26, 2009, pp. 21-30.
47. Saber, H.H., Maref, W., and Abdulghani, K., Determining through numerical modeling the effective thermal resistance of a foundation wall system with a low emissivity material bonded to thermal insulation and furred-airspace assembly – Phase II, report number B-1265.3 (A1-000440), Client Report. NRC - Construction, pp. 1-71, November, 2012.
48. Saber, H.H., Maref, W., and Abdulghani, K., Determining through numerical modeling the effective thermal resistance of a foundation wall system with a low emissivity material bonded to thermal insulation and furred-airspace assembly – Phase I, report number B-1265.2 (A1-000440), Client Report. NRC - Construction, pp. 1-111, September, 2012.
49. Saber, H.H., and Maref, W., Determining through numerical modeling the effective thermal resistance of a foundation wall system with a low emissivity material bonded to thermal

insulation and furred-airspace assembly: Model benchmarking and sensitivity analyses, Client Report. NRC Institute for Research in Construction, pp. 1-7, October 2011 (B-1265.1).

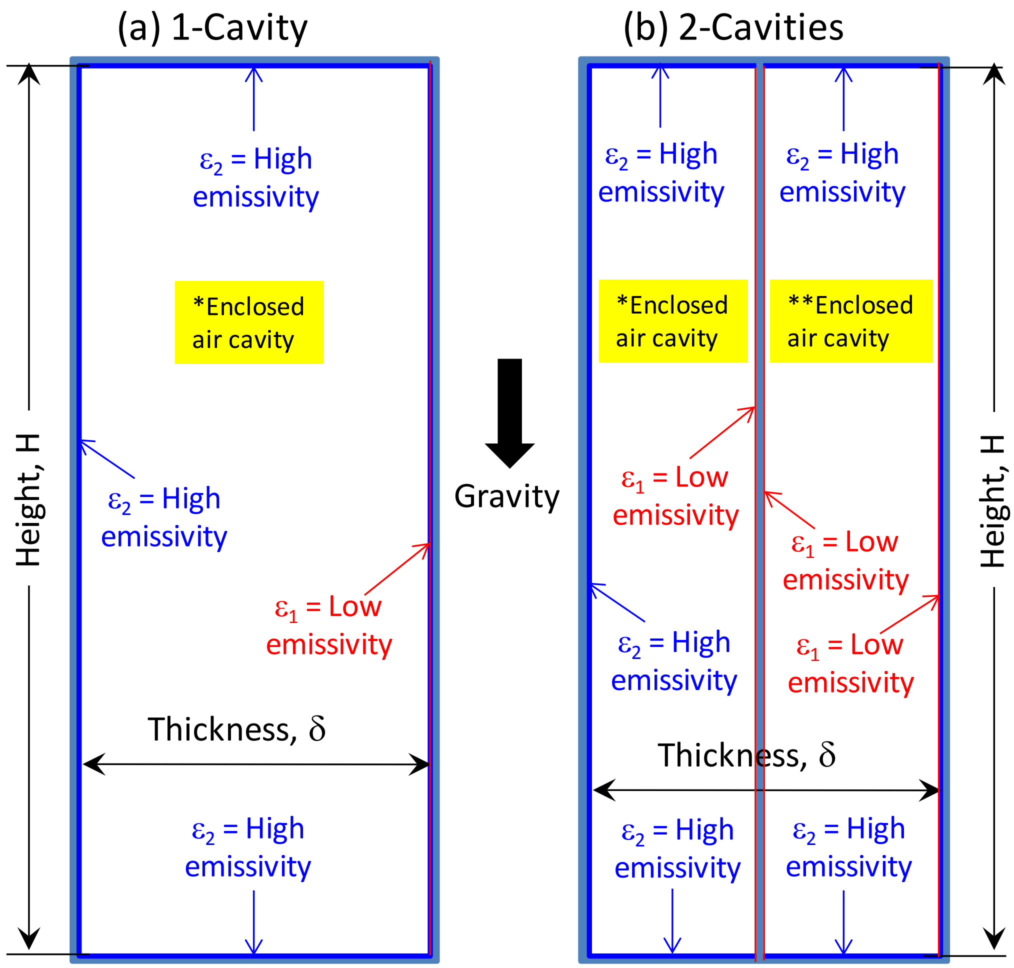

* $1/\varepsilon_{eff} = 1/\varepsilon_1 + 1/\varepsilon_2 - 1$

** $1/\varepsilon_{eff} = 2/\varepsilon_1 - 1$

Figure 1. Schematics of enclosed airspace with and without thin sheet of low emissivity on both sides, placed in the middle of the airspace.

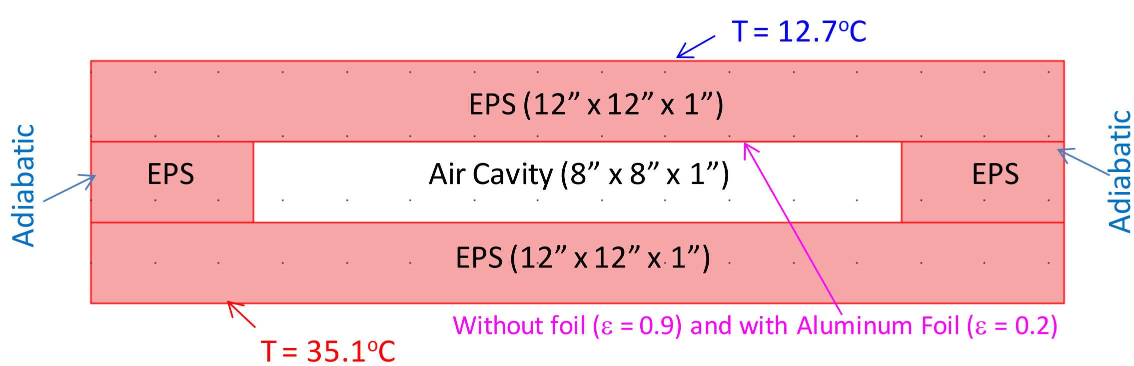

Figure 2. Sample stacks tested at NRC [23]

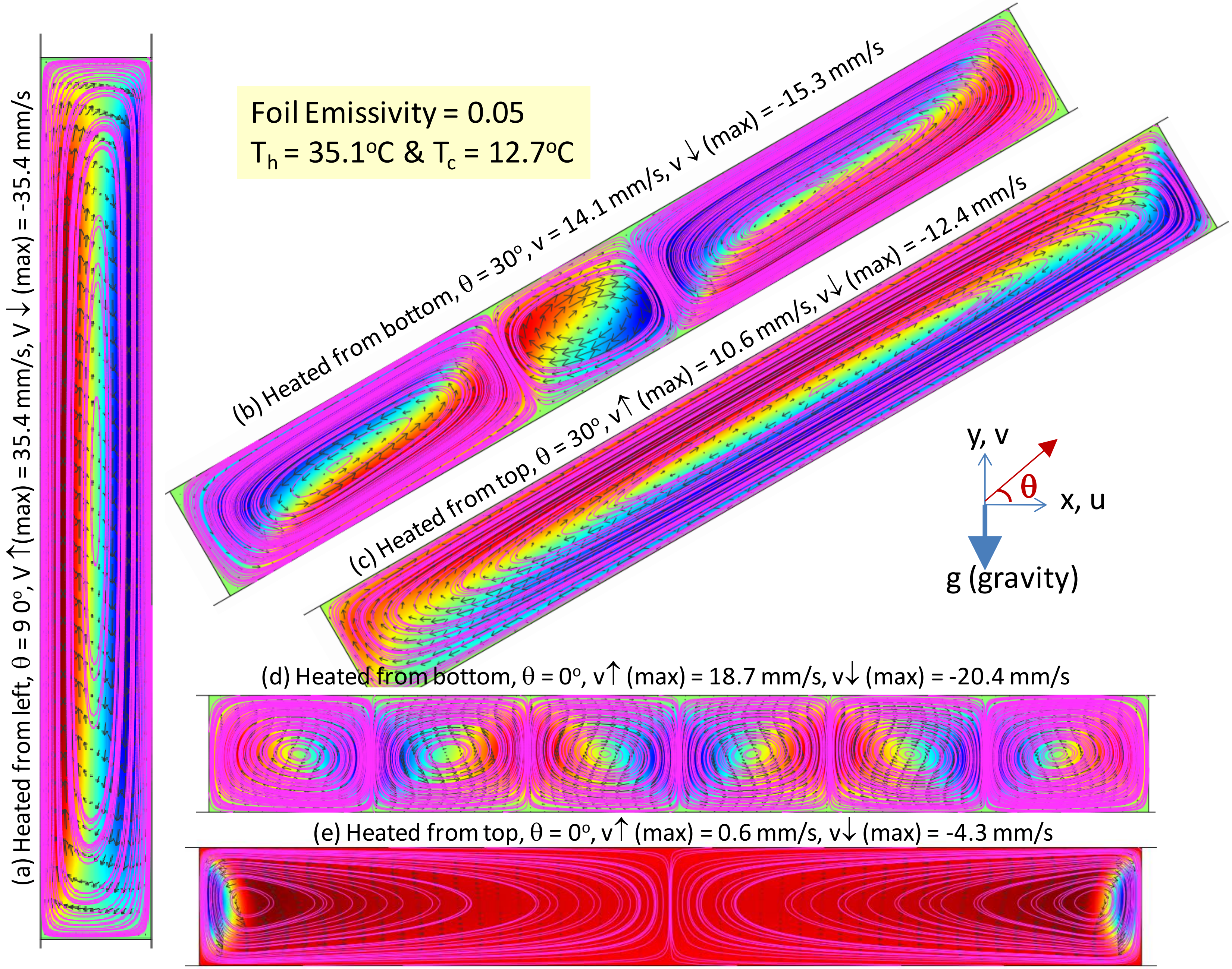

Figure 3. Vertical velocity contours and flow field in the air cavity of sample stacks with different inclinations

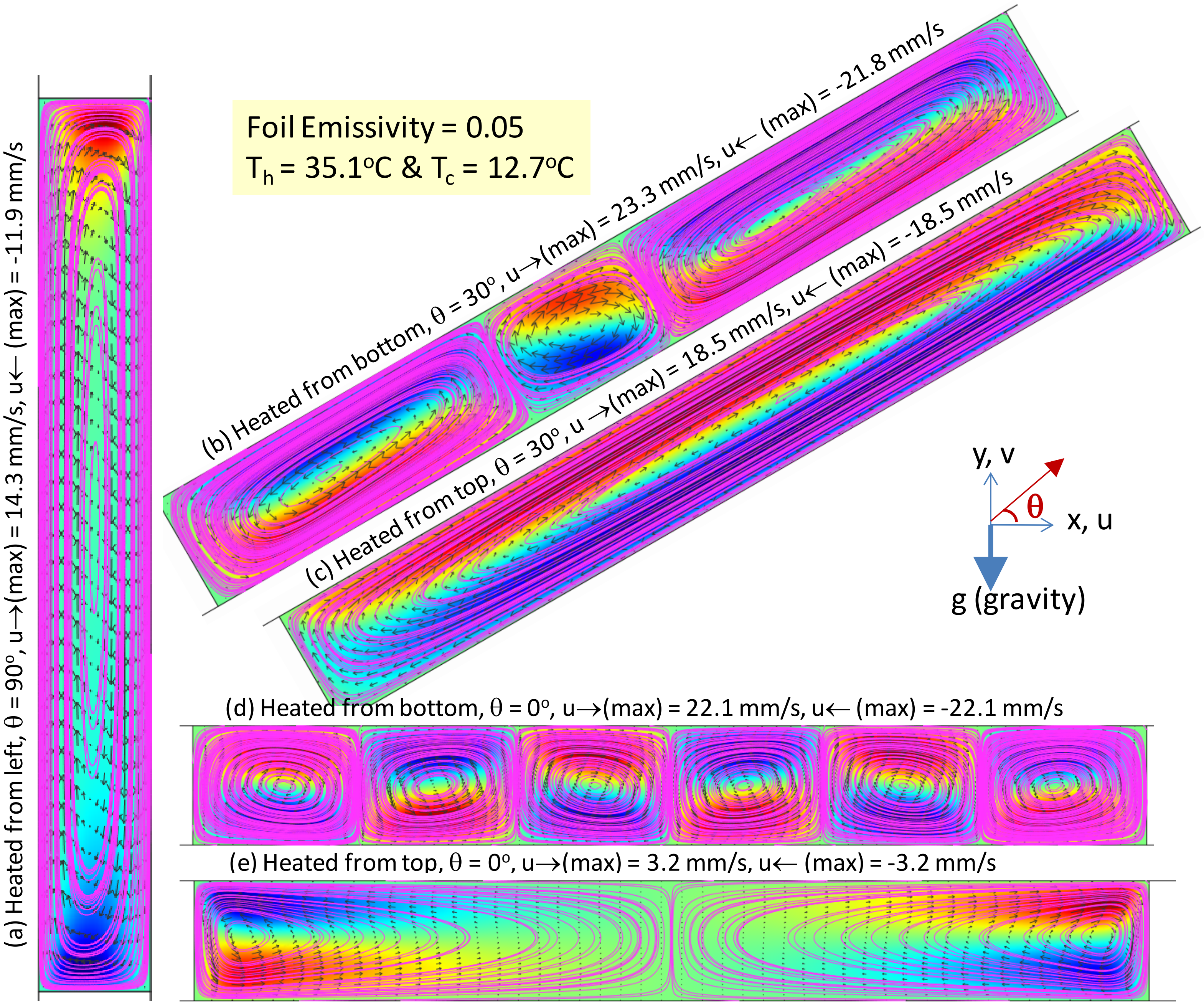

Figure 4. Horizontal velocity contours and flow field in the air cavity of sample stacks with different inclinations

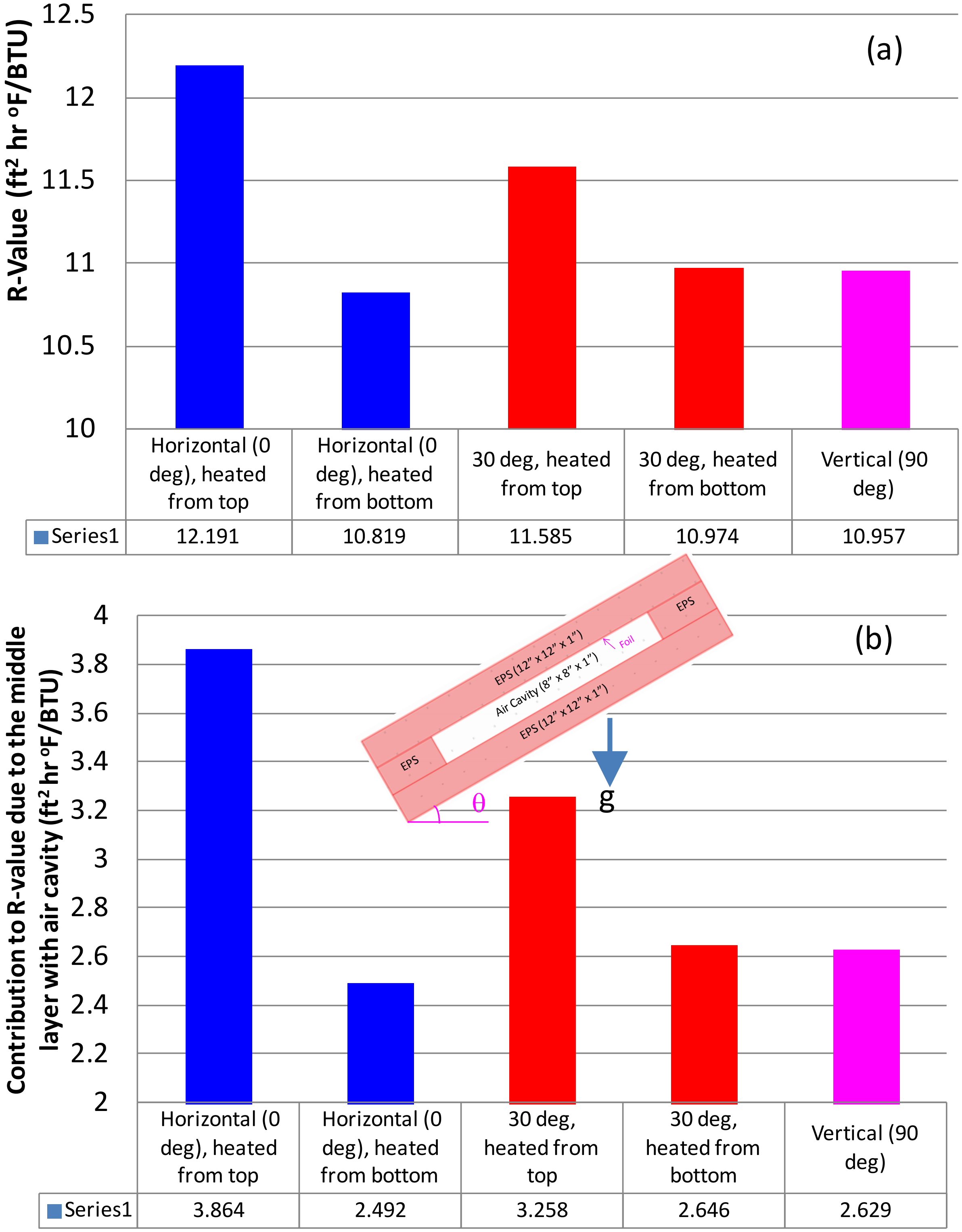

Figure 5. Effect of inclination angle of sample stack and direction of heat flow on the effective R-value in the case of foil emissivity of 0.05

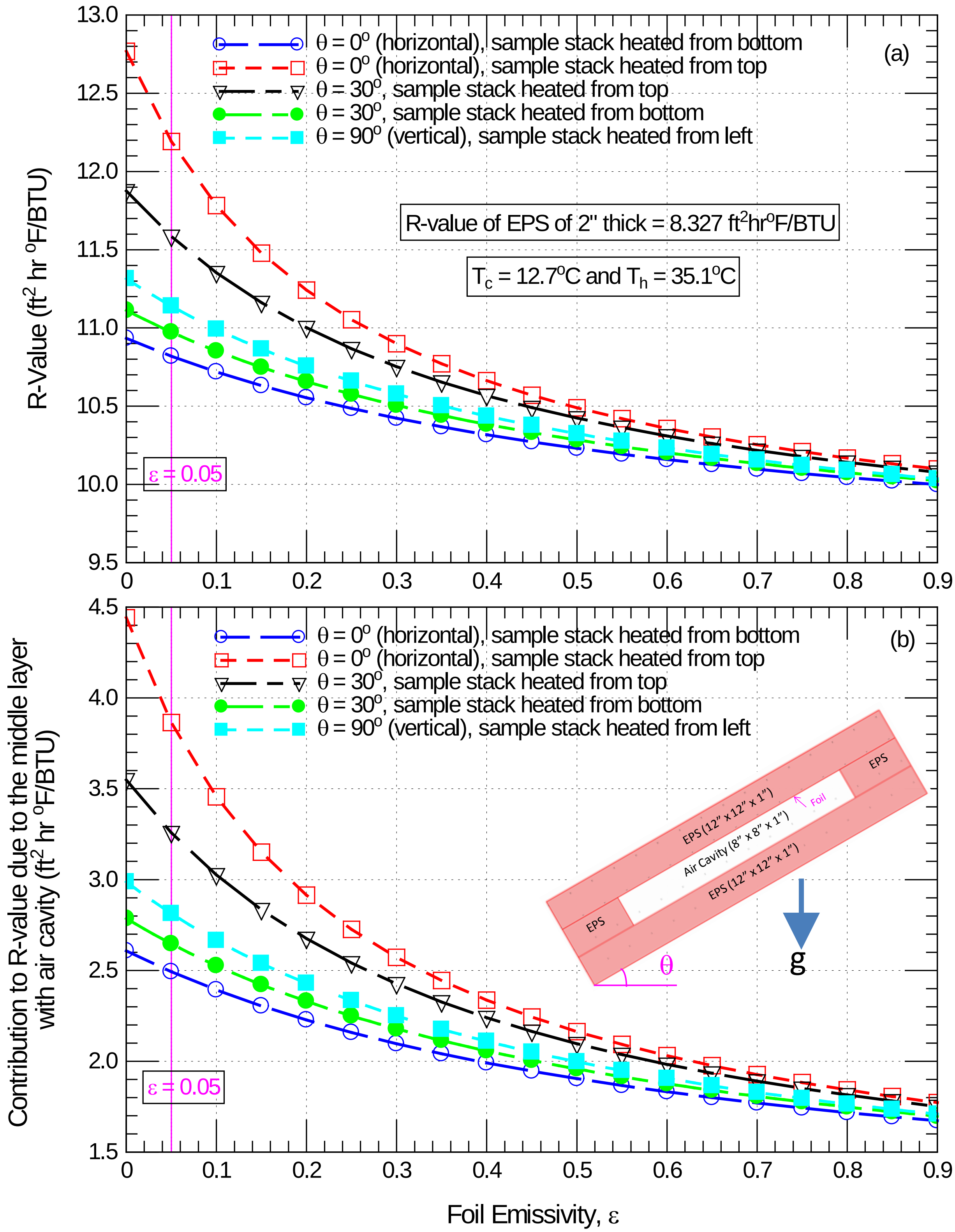

Figure 6. Effect of inclination angle of sample stack, foil emissivity and direction of heat flow on the effective R-value